PHYSICAL REVIEW D **94,** 055014 (2016)

Higgs mass and right-handed sneutrino WIMP in a supersymmetric 3 – 3 – 1 model

C. A. de S. Pires, P. S. Rodrigues da Silva, A. C. O. Santos, and Clarissa Siqueira
Departamento de Física, Universidade Federal da Paraíba, Caixa Postal 5008, 58051-970, João Pessoa, Paraíba, Brazil
(Received 6 August 2016; published 13 September 2016)

This work deals with the right-handed sneutrino as thermal cold dark matter candidate. This scalar emerges in a supersymmetric version of the $SU(3)_c \otimes SU(3)_L \otimes U(1)_X$ gauge model where right-handed neutrinos are a natural component of leptonic chiral scalar supermultiplets. We first consider the issue of a 125 GeV Higgs boson mass in this model, showing that constraints on the stop mass and trilinear soft coupling are considerably alleviated compared to the minimal supersymmetric standard model. Then, we investigate the region of parameter space that is consistent with right-handed sneutrino as thermal cold dark matter, under the light of Planck results on the relic abundance and direct detection from the LUX experiment. This sneutrino mainly annihilates through an extra neutral gauge boson, Z', and Higgs exchange so that the physics of dark matter is somewhat related to the parameters determining Higgs and Z' masses. We then obtain that the right-handed sneutrino in this model must be heavier than 400 GeV to conform with Planck and LUX, simultaneously constraining the Z' mass to be above 2400 GeV, which is in perfect agreement with LHC searches in a nonsupersymmetric version of this model.

DOI: 10.1103/PhysRevD.94.055014

I. INTRODUCTION

The amount of missing mass in the Universe, the so-called dark matter, has been precisely determined after WMAP [1] and Planck [2] satellites. However, there seems to be no real appealing solution to this problem besides it being constituted of new neutral and stable particle(s) beyond those already known. Several facilities were aimed at detecting it directly [3–6], mainly when it lies in the range of the hundreds of GeV mass scale, characterizing what is known as a weakly interacting massive particle (WIMP) [7,8]. The WIMP paradigm is so largely accepted because it miraculously fits what is expected from a natural extension of the standard model of electroweak interactions (SM), realized close to its symmetry-breaking scale, around 1 TeV, and the interactions of which are sort of weak, too, allowing for the observed abundance of cold dark matter (CDM). Concomitantly, there are strong reasons to believe that supersymmetry (SUSY) may exist at very high energies and be broken close to the electroweak scale, being phenomenologically accessible at the LHC. If SUSY is armed with R-parity symmetry for the component fields, $R = (-1)^{3(B-L)+2s}$, a discrete symmetry that may be a remnant of a $U(1)_{B-L}$ lepton-baryon number gauge symmetry, avoiding the proton decay, it simultaneously provides a stable supersymmetric particle with the right features to be a WIMP.

Among the neutral supersymmetric particles, the sneutrino [9–11] as well as neutralino [7] are the two kinds of particles that may play the role of WIMPs. However, in the minimal supersymmetric standard model (MSSM), only the neutralino is viable as a CDM candidate because the left-handed sneutrino has a sizable coupling with the Z^0 boson and, consequently, either gives a small relic abundance or is excluded by direct CDM searches [3–6]. It would be interesting to look for extensions of the MSSM that could accommodate both forms of WIMPs as viable CDM (not simultaneously though), augmenting the chances of describing it while conforming with phenomenological constraints over the model. In this direction, there is no other alternative except considering the scalar superpartner of the right-handed neutrino [12–23].

Instead of only adding a new singlet superfield to the MSSM to obtain the right-handed sneutrino, we call on the supersymmetric version of a gauge extension of the SM, the $SU(3)_C \times SU(3)_L \times U(1)_X$ $(3-3-1)$ gauge model that already possesses right-handed neutrinos as a natural ingredient of their particle content [24–26]. This class of model presents appealing features, one of them being the fact that a minimal of three families is necessary in order to cancel anomalies, offering an explanation to the old family puzzle [27,28]. They also shed some light on the understanding of the quantization of electric charges [29] and provide a solution to the strong CP problem [30–32], address the neutrino mass and oscillation pattern [33–37], possess neutral stuff that can be accommodated in a WIMP framework [38–41], can account for a possible extra radiation imprint on the cosmic microwave background radiation [42,43], etc. These features surely confer enough motivation that justifies the development of such a class of gauge models and their supersymmetric versions.[1]

[1]Although $3-3-1$ gauge models are becoming popular and very well developed, their supersymmetric versions have received scarce attention. For some works considering SUSY $3-3-1$, see Refs. [44–47].

In this work, we study the Higgs and the dark matter sector of the supersymmetric version of the $3-3-1$ model with right-handed neutrinos (S331RHν). We argue that the right-handed sneutrino, decoupled from the Z^0 gauge boson, is the simplest form of the CDM candidate provided by the model. We then calculate its relic abundance and investigate the direct detection of the sneutrino as a WIMP. To be sure that our results are realistic, we also investigate the scalar sector of the model and show that a Higgs with a mass of 125 GeV with stop mass and soft trilinear coupling below the TeV scale is a natural outcome of the model.

The paper is divided in the following way. In Sec. II, we introduce the main ingredients of the model, identifying its content, mass spectrum, superpotential, and soft SUSY-breaking terms according to the gauge and discrete symmetries imposed. Next, in Sec. III, we focus on numerical calculation of the Higgs mass in this model, looking at the leading quantum contribution. We then, in Sec. IV, analyze the sneutrino as a WIMP candidate by computing its relic abundance and direct-detection cross section, contrasting them with observation. We finally conclude in Sec. V.

II. MAIN INGREDIENTS OF THE MODEL

In the leptonic sector, the superfields of the three generations compose triplet and singlet representations according to the following transformation by the $3-3-1$ symmetry,

$$\hat{L}_a = \begin{pmatrix} \hat{\nu}_a \\ \hat{e}_a \\ \hat{\nu}_a^c \end{pmatrix}_L \sim (1,3,-1/3), \qquad \hat{l}_{aL}^c \sim (1,1,-1), \tag{1}$$

where $a = 1,2,3$ represents the family index for the usual three generations of leptons. Observe that right-handed neutrinos are incorporated as the third component of a fundamental representation of $SU(3)_L$ for leptons, while the right-handed charged leptons are singlets under this symmetry.

In the hadronic sector, the superfields of the third generation come in the triplet representation, and the superfields of the other two are in antitriplet representations of $SU(3)_L$, as a requirement for anomaly cancellation. They are given by

$$\begin{aligned} \hat{Q}_{\alpha_L} &= \begin{pmatrix} \hat{d}_\alpha \\ \hat{u}_\alpha \\ \hat{d}'_\alpha \end{pmatrix}_L \sim (3,3^*,0); \\ \hat{u}^c_{\alpha_L} &\sim (3^*,1,-2/3), \qquad \hat{d}^c_{\alpha_L}, \hat{d}'^c_{\alpha_L} \sim (3^*,1,1/3), \\ \hat{Q}_{3L} &= \begin{pmatrix} \hat{u}_3 \\ \hat{d}_3 \\ \hat{u}'_3 \end{pmatrix}_L \sim \left(3,3,\frac{1}{3}\right), \\ \hat{u}^c_{3L}, \hat{u}'^c_{3L} &\sim (3^*,1,-2/3), \qquad \hat{d}^c_{3L} \sim (3^*,1,1/3), \end{aligned} \tag{2}$$

where $\alpha = 1, 2$.

The scalars of the model, responsible for the spontaneously broken gauge symmetry, compose the superfields

$$\hat{\eta} = \begin{pmatrix} \hat{\eta}_1 \\ \hat{\eta}^- \\ \hat{\eta}_2 \end{pmatrix}, \qquad \hat{\chi} = \begin{pmatrix} \hat{\chi}_1 \\ \hat{\chi}^- \\ \hat{\chi}_2 \end{pmatrix}, \qquad \hat{\rho} = \begin{pmatrix} \hat{\rho}_1^+ \\ \hat{\rho} \\ \hat{\rho}_2^+ \end{pmatrix}, \tag{3}$$

where $\hat{\eta}, \hat{\chi} \sim (1,3,-1/3)$, $\hat{\eta} \sim (1,3,2/3)$, and

$$\hat{\eta}' = \begin{pmatrix} \hat{\eta}'_1 \\ \hat{\eta}'^- \\ \hat{\eta}'_2 \end{pmatrix}, \qquad \hat{\chi}' = \begin{pmatrix} \hat{\chi}'_1 \\ \hat{\chi}'^- \\ \hat{\chi}'_2 \end{pmatrix}, \qquad \hat{\rho}' = \begin{pmatrix} \hat{\rho}'_1{}^+ \\ \hat{\rho}' \\ \hat{\rho}'_2{}^+ \end{pmatrix}, \tag{4}$$

where $\hat{\eta}', \hat{\chi}' \sim (1,3^*,1/3)$, $\hat{\rho}' \sim (1,3^*,-2/3)$. It is opportune to remark that the nonsupersymmetric version of this model demands a total of at least three scalar triplets in order to engender spontaneous symmetry breaking and describe fermion masses. The scalars that transform in the same way ($\hat{\eta}$ and $\hat{\chi}$, for example) have different neutral components developing a vacuum expectation value (VEV) in a way that lepton number is conserved by the vacuum. This is the reason to have two such triplets. Considering this and given their quantum numbers, we are obliged to duplicate all three scalar triplets associating opposite quantum numbers to them so as to cancel gauge anomalies, justifying the choice above.

For reasons of simplicity (and avoiding spontaneous lepton-number violation), we assume that only the neutral scalars η_1, η'_1, ρ, ρ', χ_2, and χ'_2 develop nonzero VEV according to

$$\begin{aligned} \langle \eta_1 \rangle &= \frac{v_{\eta_1}}{\sqrt{2}}, \qquad \langle \eta'_1 \rangle = \frac{v_{\eta'_1}}{\sqrt{2}}, \qquad \langle \rho \rangle = \frac{v_\rho}{\sqrt{2}}, \\ \langle \rho' \rangle &= \frac{v_{\rho'}}{\sqrt{2}}, \qquad \langle \chi_2 \rangle = \frac{v_{\chi_2}}{\sqrt{2}}, \qquad \langle \chi'_2 \rangle = \frac{v_{\chi'_2}}{\sqrt{2}}. \end{aligned} \tag{5}$$

These VEVs lead to the following gauge symmetry-breaking pattern:

$$\begin{aligned} SU(3)_C \otimes SU(3)_L \otimes U(1)_X &\xrightarrow{v_{\chi_2}, v_{\chi'_2}} SU(3)_C \\ \otimes SU(2)_L \otimes U(1)_Y &\xrightarrow{v_{\eta_1}, v_{\eta'_1}, v_\rho, v_{\rho'}} SU(3)_C \otimes U(1)_{\mathrm{QED}}. \end{aligned} \tag{6}$$

With the breaking of the gauge symmetry by this set of VEVs, the expected particles, including the supersymmetric ones, receive mass. What matters for us here are the scalars' and gauge bosons' masses. Concerning the gauge bosons, they are composed by the standard gauge bosons γ, Z^0, and $W^\pm$; two new neutral massive gauge bosons Z' and U^0; and two simply charged gauge bosons $V^\pm$ with the mass expression

$$M^2_{Z^0} = \frac{g^2}{4}\frac{(3+4t^2)}{(3+t^2)}(v^2_\rho + v^2_{\rho'} + v^2_{\eta_1} + v^2_{\eta'_1}), \quad (7)$$

$$M^2_{Z'} = \frac{g^2}{9}(3+t^2)(v^2_{\chi_2} + v^2_{\chi'_2}), \quad (8)$$

$$M_{U^0} = \frac{g^2}{4}(v^2_\rho + v^2_{\rho'} + v^2_{\chi_2} + v^2_{\chi'_2}), \quad (9)$$

$$M_{W^\pm} = \frac{g^2}{4}(v^2_\rho + v^2_{\rho'} + v^2_{\eta_1} + v^2_{\eta'_1}), \quad (10)$$

$$M_{V^\pm} = \frac{g^2}{4}(v^2_{\eta_1} + v^2_{\eta'_1} + v^2_{\chi_2} + v^2_{\chi'_2}), \quad (11)$$

where $t = g_N/g$, $v^2_\rho + v^2_{\rho'} + v^2_{\eta_1} + v^2_{\eta'_1} = v^2_{ew}$ and $v^2_{\chi_2} + v^2_{\chi'_2} \equiv v^2_\chi$ with v_χ lying in the TeV scale.

On imposing the standard relation,

$$\frac{M^2_{Z^0}}{M^2_{W^\pm}} = \frac{(3+4t^2)}{(3+t^2)} = \frac{1}{\cos^2\theta_W}, \quad (12)$$

we obtain

$$t^2 = \frac{\sin^2\theta_W}{1 - 4/3\sin^2\theta_W}, \quad (13)$$

where θ_W is the electroweak mixing angle. In addition, the mixing between the neutral gauge bosons is given by[2]

$$W_N = \frac{\sqrt{3}}{\sqrt{3+4t^2}}\gamma - \frac{3t}{\sqrt{3+4t^2}\sqrt{3+t^2}}Z^0 + \frac{t}{\sqrt{3+t^2}}Z', \quad (14)$$

$$W_8 = -\frac{t}{\sqrt{3+4t^2}}\gamma + \frac{\sqrt{3}t^2}{\sqrt{3+4t^2}\sqrt{3+t^2}}Z^0 + \frac{\sqrt{3}}{\sqrt{3+t^2}}Z', \quad (15)$$

$$W_3 = \frac{\sqrt{3}t}{\sqrt{3+4t^2}}\gamma + \frac{\sqrt{3+t^2}}{\sqrt{3+4t^2}}Z^0. \quad (16)$$

To work in the minimal scenario, we assume R-parity conservation and invariance by a Z_2 symmetry with the following superfields transforming nontrivially under Z_2: $(\hat{l}^c, \hat{d}^c, \hat{u}^c, \hat{\rho}, \hat{\rho}', \hat{\eta}, \hat{\eta}') \to -(\hat{l}^c, \hat{d}^c, \hat{u}^c, \hat{\rho}, \hat{\rho}', \hat{\eta}, \hat{\eta}')$. This set of symmetries allows us to work with a shortened superpotential that is formed by the terms

$$\begin{aligned} W_{331} = {} & \lambda^l_{ij}\hat{L}_i\hat{\rho}'\hat{l}^c_j + \lambda^d_{\alpha i}\hat{Q}_\alpha\hat{\eta}\hat{d}^c_{i_L} + \lambda^d_{3i}\hat{Q}_3\hat{\rho}'\hat{d}^c_{i_L} + \lambda^u_{\alpha_i}\hat{Q}_\alpha\hat{\rho}\hat{u}^c_{i_L} \\ & + \lambda^u_{3i}\hat{Q}_3\hat{\eta}'\hat{u}^c_{i_L} + \lambda'_{\alpha\beta}\hat{Q}_\alpha\hat{\chi}\hat{d}'^c_{\beta_L} + \lambda'_{33}\hat{Q}_3\hat{\chi}'\hat{u}'^c_{3_L} \\ & + f_1\varepsilon_{ijk}\hat{\eta}'_i\hat{\rho}'_j\hat{\chi}'_k + f_2\varepsilon_{ijk}\hat{\eta}_i\hat{\rho}_j\hat{\chi}_k \\ & + \mu_\eta\hat{\eta}\hat{\eta}' + \mu_\rho\hat{\rho}\hat{\rho}' + \mu_\chi\hat{\chi}\hat{\chi}' + \text{H.c.}, \end{aligned} \quad (17)$$

where $\alpha, \beta = 1, 2$ and $i, j, k = 1, 2, 3$.

Until this point, the masses of the ordinary particles are equal to the masses of their superpartners. As usual in phenomenological supersymmetric models, SUSY must be broken so as to provide a reasonable shift between ordinary particles and their supersymmetric partners. In this work, we assume that SUSY is broken explicitly through the set of soft breaking terms that are invariant under the symmetries assumed here,

$$\begin{aligned} \mathcal{L}_{\text{Soft}} = {} & -\frac{1}{2}\left[m_{\lambda_G}\sum_{b=1}^{8}(\bar{\lambda}^b_G\lambda^b_G) + m_{\lambda_W}\sum_{b=1}^{8}(\bar{\lambda}^b_W\lambda^b_W) + m_{\lambda_X}\bar{\lambda}_X\lambda_X + \text{H.c.}\right] + m^2_L\tilde{L}^\dagger\tilde{L} + m^2_l\tilde{l}^\dagger_i\tilde{l}_i + m^2_{Q_3}\tilde{Q}_3{}^\dagger\tilde{Q}_3 \\ & + m^2_{Q_\alpha}\tilde{Q}_\alpha{}^\dagger\tilde{Q}_\alpha + m^2_{u_i}\tilde{u}_i{}^\dagger\tilde{u}_i + m^2_{u_i}\tilde{u}_i{}^\dagger\tilde{u}_i + m^2_{d_i}\tilde{d}_i{}^\dagger\tilde{d}_i + m^2_{u'}\tilde{u'}^\dagger\tilde{u'} + m^2_{d'_\alpha}\tilde{d}'^\dagger_\alpha\tilde{d}'_\alpha - m^2_\eta\eta^\dagger\eta - m^2_\rho\rho^\dagger\rho \\ & - m^2_\chi\chi^\dagger\chi - m^2_{\eta'}\eta'^\dagger\eta' - m^2_{\rho'}\rho'^\dagger\rho' - m^2_{\chi'}\chi'^\dagger\chi' + y^l_{ij}\tilde{L}_i\rho\tilde{l}^c_{j_L} + y^d_{\alpha i}\tilde{Q}_\alpha\eta\tilde{d}^c_{i_L} + y^d_{3i}\tilde{Q}_3\rho'\tilde{d}^c_{i_L} + y^u_{\alpha i}\tilde{Q}_\alpha\rho\tilde{u}^c_{i_L} \\ & + y^d_{\alpha i}\tilde{Q}_\alpha\eta\tilde{d}^c_{i_L} + y^u_{3i}\tilde{Q}_3\eta'\tilde{u}^c_{i_L} + y'_{\alpha i}\tilde{Q}_\alpha\chi\tilde{d}'^c_{i_L} + y^u_{33}\tilde{Q}_3\chi'\tilde{u}'^c{}_{3_L} - [k_1\varepsilon_{ijk}\eta_i\rho_j\chi_k + k_2\varepsilon_{ijk}\eta'_i\rho'_j\chi'_k + \text{H.c.}] \\ & + b_\eta\eta'\eta + b_\chi\chi'\chi + b_\rho\rho'\rho, \end{aligned} \quad (18)$$

where λ^b_G are the gluinos; λ^b_W are gauginos associated to $SU(3)_L$ (in both cases, b is the gauge group index); λ_X is the gaugino associated to $U(1)_X$; scalar supersymmetric partners of fermion fields, f, are denoted by $\tilde{f}$; and the remaining fields are self-evident.

Once we have settled the interactions and parameters of the S331RHν model, we are then ready to start the development of the main proposal of this work that is to check if the R-sneutrino of the model is a good CDM. But first, we study the possible range of parameters that can

[2]Provided that the mixing among Z^0 and Z' is very small [48], we neglect such mixing throughout this work.

explain the observed 125 GeV Higgs mass. This will constrain the parameters that will be used in the CDM analysis.

III. HIGGS MASS: NUMERICAL RESULTS

In this section, we obtain the mass of the lightest CP-even neutral scalar provided by the model, which we assume is the Higgs boson. First of all, we have to obtain the scalar potential, which is composed of $V = V_F + V_D + V_{\text{soft}}$, where V_F and V_D are the F-term and D-term, respectively, and V_{soft} comes from the soft SUSY-breaking terms. With the potential in hand, we are ready to obtain the minimum conditions over the potential which translate to a set of constraint equations, $\frac{\partial V}{\partial \phi_i}|_{\phi_i=\langle\phi_i\rangle_0} = 0$, where $\phi_i = \langle\phi_i\rangle_0$ means that all scalar fields are computed at their VEV. The squared mass matrix can then be built by taking $\frac{\partial^2 V}{\partial\phi_a\partial\phi_b}|_{\phi_i=\langle\phi_i\rangle_0}$. Finally, by applying the set of minimum conditions over the mass matrices and diagonalizing them, we obtain the physical scalars of the model. Because of the complexity of V, we are not showing here the analytical expressions for $\frac{\partial V}{\partial\phi_i}|_{\phi_i=\langle\phi_i\rangle_0} = 0$ and $\frac{\partial^2 V}{\partial\phi_a\partial\phi_b}|_{\phi_i=\langle\phi_i\rangle_0}$, which are not illuminating at all. We then proceed with a numerical approach to diagonalize the mass matrices in question. For this, we made use of a subroutine called jacobi [49], which composes the micrOMEGAs package [50,51]. This is enough to develop the features of the model we are interested in.

The CP-even neutral scalar fields compose a 10×10 mass matrix. However, the neutral scalars $\eta_2, \eta_2', \chi_1, \chi_1'$ carry two units of lepton number, and as far as lepton number is conserved, they decouple from the other six neutral scalars. On diagonalizing the remaining 6×6 mass matrix, we obtain six physical CP-even neutral scalars. Two of them, which is a combination mainly of χ_2 and χ_2', are very heavy with mass at the $3-3-1$ scale, typically around few TeV. The other four, which are mainly combinations of η_1 η_1', ρ, and ρ', acquire masses at electroweak scale with the lightest of them being the Higgs. We refer to these four scalars as h (the Higgs boson), h', H, and H'.

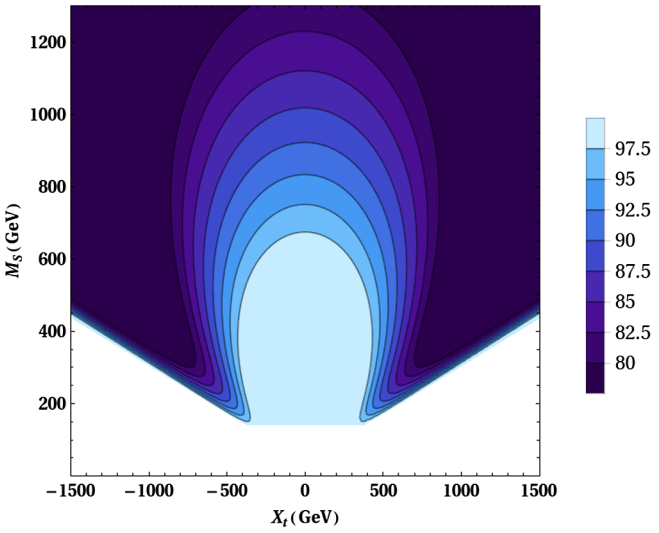

FIG. 1. Contour plot corresponding to $m_h = 125$ GeV in the M_s vs the X_t plane where $m_t = 173$ GeV and $v_{ew} = 246$ GeV. The legend bar indicates the range of values provided solely by the tree-level mass.

In what follows, we present the results only for the lightest CP-even scalar, the Higgs boson. For this, we choose as independent parameters the set of variables

$$\begin{aligned}
0.0001 \le |f_1, f_2| &\le 0.0049,\\
8\ \text{GeV} \le |k_1, k_2| &\le 15\ \text{GeV},\\
400\ \text{GeV} \le |\mu_\eta, \mu_\rho| &\le 700\ \text{GeV},\\
800\ \text{GeV} \le |\mu_\chi| &\le 10000\ \text{GeV},\\
300\ \text{GeV}^2 \le |b_\eta, b_\rho| &\le 500\ \text{GeV}^2,\\
50000\ \text{GeV}^2 \le |b_\chi| &\le 100000\ \text{GeV}^2,\\
40 \le v_{\eta_1} &\le 140\ \text{GeV},\\
30\ \text{GeV} \le v_{\eta_1'}, v_{\rho'} &\le 50\ \text{GeV},\\
5000\ \text{GeV} \le v_{\chi_2} &\le 10000\ \text{GeV},\\
700\ \text{GeV} \le v_{\chi_2'} &\le 2000\ \text{GeV},
\end{aligned} \tag{19}$$

where their range of values to be scanned in the numerical computation were fixed so as to guarantee the scalar potential stability, while there is a constraint among some of the VEVs,

$$v_\rho^2 + v_{\eta_1}^2 + v_{\eta_1'}^2 + v_{\rho'}^2 = (246\ \text{GeV})^2,$$

which comes from the known $W^\pm$ mass.

From the numerical diagonalization of the 6×6 mass matrix, we obtain that the lightest CP-even neutral scalar gains mass at tree level in the range from 80 to 100 GeV. Considering that in the MSSM the maximal value the Higgs mass may attain at tree level is 91 GeV, we have that the S331RHν model provides a better tree-level contribution to the Higgs mass. However, loop corrections to the Higgs mass are still necessary. At this point, we just consider the leading one-loop correction for the Higgs mass dictated by the MSSM of which the expression is[3]

$$\Delta m_h^2 = \frac{3m_t^4}{2\pi^2 v_{ew}^2}\left(\log\left(\frac{M_s^2}{m_t^2}\right) + \frac{X_t^2}{M_s^2}\left(1 - \frac{X_t^2}{12M_s^2}\right)\right), \tag{20}$$

where m_t is the top mass, $v_{ew} = 246$ GeV is the standard electroweak VEV, X_t is the soft trilinear coupling of the

[3]While the S331RHν model contains the MSSM, justifying this approximation, we remark that a finer computation can be pursued not only by including full two-loop effects [52] but also the new contributions specific from the enlarged particle spectrum of the model.

stops, and $M_s \equiv (m_{\tilde{t}_1} m_{\tilde{t}_2})^{1/2}$ is the SUSY scale (scale of superpartners masses) where $m_{\tilde{t}}$ is the stops' mass, that we suppose to be degenerated.

We add this one-loop contribution to the tree level Higgs mass and then perform the scan on the parameter space. Our results are shown in Fig. 1.

It is remarkable that the S331RHν model is able to yield a tree-level Higgs mass around 100 GeV (the lightest blue in Fig. 1), where stop mass, $m_{\tilde{t}}$, below TeV along with a small X_t are enough to generate the necessary radiative corrections to produce the observed Higgs mass at one loop in the approximation where only stops were taken into account. In other words, differently from the MSSM where $m_{\tilde{t}}$ is pushed beyond 1 TeV and X_t is rather large, there are no tight constraints on these parameters in the S331RHν model, which can easily accommodate a 125 GeV Higgs mass.

This result is not a surprise at all. Extensions of the MSSM that present cubic invariant terms in the superpotential generate new contributions to the Higgs potential of the MSSM which, consequently, result in new corrections at tree level to the Higgs mass. For example, in the Next to minimal supersymmetric standard model, the superfield singlet $\hat{\phi}$ is added to the MSSM superfield content and composes with the standard superfields $\hat{H}_u$ and $\hat{H}_d$ the following invariant cubic term $\lambda \hat{H}_u \hat{H}_d \hat{\phi}$ in the superpotential of the model. Such a term furnishes an additional tree-level correction to the Higgs mass expression of the MSSM which makes it possible to lift the Higgs mass by some units of GeV, which is sufficient to alleviate the tension on the quantum corrections involving stops [53]. Another example is the extension of the MSSM with the superfiled triplets $\hat{\Delta}_1$ and $\hat{\Delta}_2$. In this case, the cubic invariant terms $\lambda_1 \hat{H}_u \hat{\Delta}_1 \hat{H}_u + \lambda_2 \hat{H}_d \hat{\Delta}_2 \hat{H}_d$ compose the superpotential of the model and provide robust tree-level corrections to the Higgs mass [54]. In the particular case of $3-3-1$ models, the Higgs sector usually involves three Higgs triplets. When this is the case, cubic invariant terms as f_1 and f_2 given in Eq. (17) compose the superpotential of the supersymmetric versions of these models. Consequently these terms will generate new corrections at tree level to the Higgs mass predicted by the MSSM. This was first perceived in Ref. [55]. Our numerical approach here is in agreement with such predictions.

Once we are sure that our model recovers the observed Higgs boson mass, we are then ready to examine if $\tilde{\nu}_R$ is viable as CDM candidate. We do this in the next section.

IV. RELIC ABUNDANCE AND DIRECT DETECTION

In a SUSY model where R-parity is conserved, the lightest supersymmetric particle (LSP) is the natural candidate for CDM [7,8]. In the MSSM, the CDM may be a scalar; the superpartner of the left-handed neutrino, $\tilde{\nu}_L$; or a combination of Majorana fermionic superpartners of the scalars and the Z boson, the neutralinos. However, we already pointed out the reason why $\tilde{\nu}_L$ is not a viable CDM candidate, and then the MSSM inevitably offers only neutralinos to play this role.

Nevertheless, extensions or variants of the MSSM do allow sneutrinos as CDM, which happens when right-handed neutrinos are somehow part of the field content to be supersymmetrized [12–23]. In this case, generally, a mixing among right-handed and left-handed sneutrinos may be the LSP and constitute the CDM candidate.

In the S331RHν model, in addition to $\tilde{\nu}_L$ and neutralinos, we have a third possibility in the form of a scalar right-handed neutrino (or simply R-sneutrino), $\tilde{\nu}_R$, which emerges naturally in this model as the third component in the leptonic triplet of $SU(3)_L$. Since the $SU(2)_L$ subgroup of $SU(3)_L$ contains the matter content of MSSM, the same conclusions over the CDM candidates derived there apply to the $\tilde{\nu}_L$ in our model. We are then left with neutralinos or an R-sneutrino, which possibly can play the CDM role. Both were already investigated in a similar SUSY model with different scalar content and assumptions in Refs. [56,57]. Besides, their analysis on the R-sneutrino was taken considering it as self-interacting dark matter and cannot be compared with ours. There is a reasonable complication in our neutralino spectrum compared to the MSSM, which is related to the larger Higgsino as well as gaugino spectrum of the S331RHν model, as can be seen from Eqs. (3), (4), and (7). The resulting neutralino mass eigenstate amounts to diagonalizing a 15×15 mass matrix in contrast to the 4×4 mass matrix of the MSSM. In this work, we are not considering the neutralinos as CDM, though. Instead, our interest is driven to the LSP as the R-sneutrino.

In what concerns $\tilde{\nu}_R$, we stress that in the S331RHν model as well as in the MSSM neutrinos gain mass through effective operators. The gauge and discrete, Z_2, symmetries assumed in this work allow for the effective operators

$$\frac{\lambda^{\nu_L}}{\Lambda}(\hat{L}\hat{\eta}')(\hat{\eta}'\hat{L}) + \frac{\lambda^{\nu_R}}{\Lambda}(\hat{L}\hat{\chi}')(\hat{\chi}'\hat{L}) \tag{21}$$

as a source of neutrino masses, where λ^{ν_L} and λ^{ν_R} are dimensionless parameters and Λ is a grand unification mass scale.[4] Notice that the first effective operator engenders a mass term to the ν_L, since only the scalar component η_1' of $\hat{\eta}'$ develops a VEV, while the second operator gives mass to ν_R, in this case because only the χ_2' scalar component of $\hat{\chi}'$ develops a VEV. This implies that the left-handed neutrinos do not mix with the right-handed ones. Also, they are completely sterile in relation to the standard gauge boson interactions as they interact solely with the gauge bosons of

[4]In the numerical computations, we will take the R-sneutrino mass as a free parameter, varying other parameters like soft masses and VEVs that constrain the former ones in order to obtain the correct active neutrinos' masses.

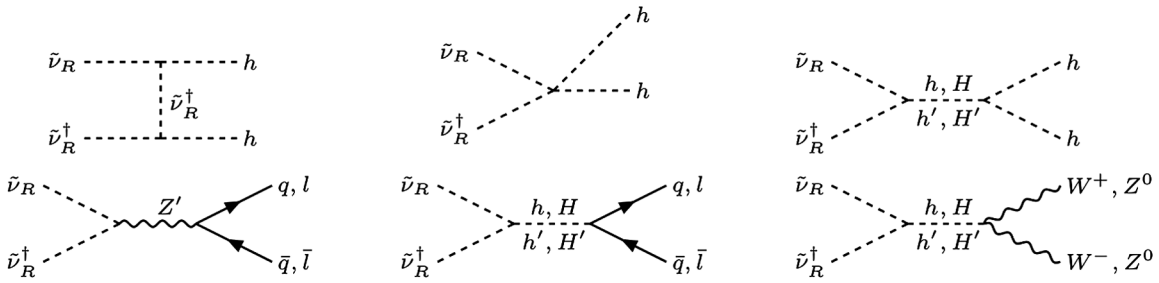

FIG. 2. Dominant processes contributing to the R-sneutrino abundance. q and l mean quarks and leptons, respectively.

the $3-3-1$ symmetry, namely, $V^{\pm}$, Z', and U^0. These properties are inherited by R-sneutrinos, and consequently, $\tilde{\nu}_R$ also does not mix with $\tilde{\nu}_L$. Besides, the bridge between them and SM particles is made through Z' and the scalars. All these features make $\tilde{\nu}_R$ rather distinct from the usual MSSM extensions where the R-sneutrino is the CDM candidate, justifying and further motivating our analysis of $\tilde{\nu}_R$ in this context. Finally, it is important to say that, as far as we know, this is the first time that $\tilde{\nu}_R$ is considered as a WIMP in the framework of the S331RHν model. We compute its relic abundance and direct-detection constraints in the following subsections.

A. Relic abundance

It is well known that the relic abundance of a WIMP is directly related to its thermal averaged annihilation cross section at the time of freeze-out [7,8]. Its decoupling is roughly determined when the interaction rate drops below the expansion rate of the Universe. To obtain the WIMP's abundance, we have to solve the Boltzmann equation,

$$\frac{dY}{dT} = \sqrt{\frac{\pi g_*(T)}{45}} M_p - \langle \sigma v \rangle (Y^2 - Y_{\rm eq}^2), \tag{22}$$

which gives the evolution of the abundance of a generic species in the Universe. In it, Y is the relic abundance as a function of the temperature, T, of the thermal bath; $Y_{\rm eq}$ is the thermal equilibrium abundance; g_* is the effective number of degrees of freedom at thermal equilibrium; and M_p is the Plank mass. $\langle \sigma v \rangle$ is the thermal averaged cross section for WIMP annihilation, with v the relative velocity between the annihilating particles. It is in this cross section that the particle physics modeling gets into the scene, and its expression can be written as [50,51]

$$\langle \sigma v \rangle = \frac{\sum_{i,j} g_i g_j \int_{(m_i+m_j)^2} ds \sqrt{s} K_1(\frac{\sqrt{s}}{T}) p_{ij}^2 \sum_{k,l} \sigma_{ij;kl}(s)}{2T(\sum_i g_i m_i^2 K_2(m_i/T))^2}, \tag{23}$$

where g_i is the number of degrees of freedom of the species involved, $\sigma_{ij;kl}$ is the total cross section for annihilation of a pair of particles with masses m_i, m_j into some SM particles (k, l) of masses m_k, m_l; p_{ij} is the momentum of incoming particles in their center-of-mass frame, with squared total energy, s; and the functions K_1 and K_2 are modified Bessel functions of first and second kinds, respectively.

The relic density is obtained integrating from $T = \infty$ to $T = T_0$, where T_0 is the temperature of the Universe today, precisely measured by the cosmic microwave backgraound radiation spectrum [1,2]. It can be cast as [50,51]

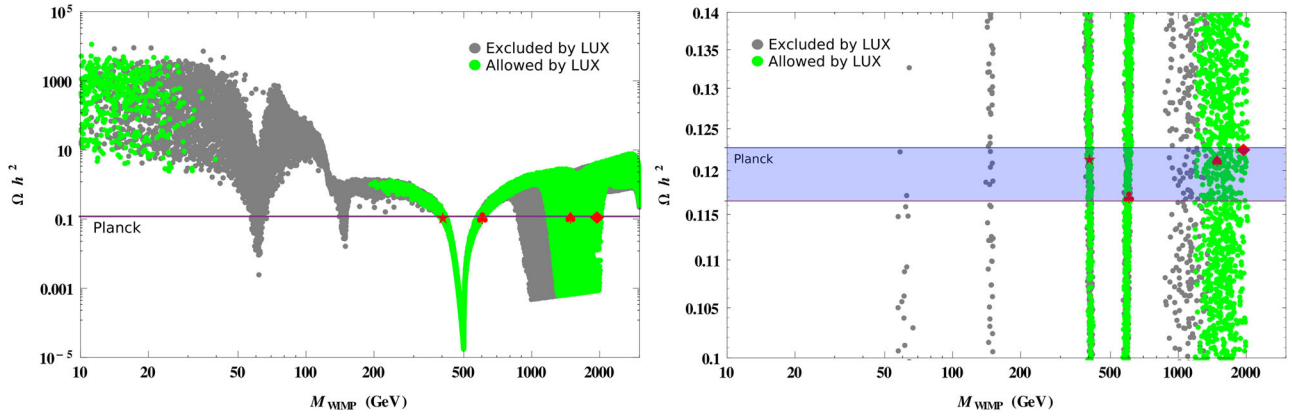

FIG. 3. Relic density vs WIMP mass. The right panel is an improvement in resolution around the Planck bounds. The gray dots are ruled out by direct-detection data. The green dots are in accordance with LUX bounds [6], while the region enclosed by purple lines represents the Planck constraints (blue shaded region on the right panel) [2].

TABLE I. In this table, we show some points with specific values for parameters of the model and the dominant channels.

Symbol	$M_{\tilde{\nu}_R}$ (GeV)	Ωh^2	$\sigma_{\tilde{\nu}_R - n}$ (pb)	$M_{Z'}$ (GeV)	Main channels
★	400	0.1215	4.041×10^{-9}	3630	$\tilde{\nu}_R,\ \tilde{\nu}_R \overset{h',H'}{\rightarrow} W^{\pm},\ Z^0,\ Z^0$
♣	600	0.1171	4.249×10^{-9}	3597	$\tilde{\nu}_R,\ \tilde{\nu}_R \overset{h',H'}{\rightarrow} W^{\pm},\ Z^0,\ Z^0$
♠	1480	0.1213	5.463×10^{-9}	3400	$\tilde{\nu}_R,\ \tilde{\nu}_R \overset{Z'}{\rightarrow} \bar{q},\ q$
◆	1934	0.1226	3.400×10^{-9}	3819	$\tilde{\nu}_R,\ \tilde{\nu}_R \overset{Z'}{\rightarrow} \bar{q},\ q$

$$\Omega h^2 = 2.742 \times 10^8 \frac{M_{\mathrm{WIMP}}}{\mathrm{GeV}} Y(T_0). \tag{24}$$

Given the large amount of interactions and mass diagonalization required in the model, an analytical approach to computing the relic abundance is unfeasible. Instead, we opt for a numerical computation using the following codes: LanHEP [58] to generate the Feynman rules in a CalcHEP [59] output to be called in micrOMEGAs [50,51]. The micrOMEGAs code is very useful in computing the CDM abundance, including coannihilation. In addition, by means of CalcHEP, it allows us to calculate the CDM scattering cross section normalized to the nucleon, so we can compare with exclusion plots given by recent direct-detection experiments [3–6].

From now on, for simplicity, we will assume that right-handed neutrinos and sneutrinos are in a diagonal basis and will consider that the lightest of the R-sneutrinos is our WIMP. We start by presenting the main channels involved in the CDM annihilation cross section, where the relevant interactions are mediated by Higgs and Z', as can be seen in Fig. 2.

In Fig. 3, we show the results of the R-sneutrino relic density. Observing the dips in the scatter plot presented in the left panel, one clearly recognizes the resonances, h, H, h', H', and Z', the masses of which are $m_h = 125$ GeV, $m_H = 300$ GeV, $m_{h'} = m_{H'} = 1000$ GeV, and 2000 GeV $< m_{Z'} < 4000$ GeV, respectively (these phenomenological reasonable values for the heavier scalars were fixed for simplicity, although they could also be varied). In the right panel, we show the same results as the left panel but zoomed in the region in the vicinity of the relic density as observed by the Planck satellite [2]. In these plots, we have included the direct-detection results provided by LUX [6], which are going to be better explained in the next section. The gray region is excluded, and the green region is allowed by LUX results. In addition, to provide the precise values of the parameters involved in the process and the dominant channels in different DM mass regions, four benchmark points were included in all plots, given by Table I, all in agreement with the constraints mentioned before.

In principle, we have four possible regions providing the correct abundance, where the WIMP mass prefers take the values 60,[5] or 500 GeV. It may also prefer to lie into the range 1000 and 2000 GeV. However, when we take into account the direct-detection bounds the WIMP mass prefers lie around 500 GeV (scalar resonances) or between 1000 and 2000 GeV (Z' resonance).

In the next section, we will detail the CDM scattering cross section to the nucleon and show the results obtained for our model including the complementary CDM relic density.

B. Direct detection

It is a well-motivated hope that, generally, any possible CDM candidate may interact with the target nuclei (more specifically the nucleons) of the detectors. These interactions may be axial, referred as spin-dependent interactions, or scalar- and/or vectorlike, known as spin-independent interactions (SI). In our model, the principal channels providing considerable direct-detection rates are given by Higgs particles and Z' (see Fig. 4), meaning we have just SI interactions.

The effective Lagrangian for SI contributions is given by

$$\mathcal{L} \supset \alpha_q^S \tilde{\nu}_R^\dagger \tilde{\nu}_R \bar{q} q + \alpha_q^V \tilde{\nu}_R^\dagger \partial_\mu \tilde{\nu}_R \bar{q} \gamma^\mu q, \tag{25}$$

with the couplings α_q^S and α_q^V depending on the parameters of the model. The WIMP-nucleus cross section that can be derived from this Lagrangian is [50]

$$\sigma_0 = \frac{4\mu_N^2}{\pi} [Z f^p + (A - Z) f^n]^2, \tag{26}$$

where μ_N is the WIMP-nucleus reduced mass, Z is the number of protons, and A is the number of nucleons. The function $f^{p,n}$ is the WIMP-nucleon amplitude that carries the particle physics model information which, for the proton, is given by[6]

[5]Such a low mass would be ruled out by the preference of the Higgs to decay into two WIMPs in this model, as could be directly inferred from the investigation in Ref. [40].

[6]We restrict ourselves to the scalar interaction since the experimental results are parametrized by this contribution to the WIMP-nucleon cross section.

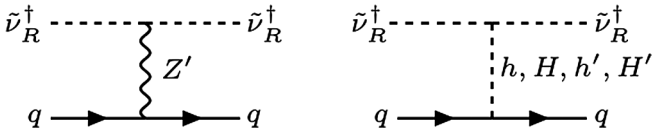

FIG. 4. Dominant processes to the WIMP-nucleon scattering cross section.

$$\frac{f^p}{m_p} = \sum_{q=u,d,s} \frac{\alpha_q^S}{m_q} f_{Tq}^p + \frac{2}{27} f_{TG}^p \sum_{q=c,b,t} \frac{\alpha_q^S}{m_q}, \tag{27}$$

where the coefficients f_{Tq}^p and f_{TG}^p are the contributions of light quarks to the proton mass, $m_p f_{Tq}^p = \langle p|m_q \bar{q} q|p\rangle$, and the WIMP-gluon interaction through quark loops, respectively, with $f_{TG}^p = 1 - \sum_{q=u,d,s} f_{Tq}^p$. Experimentally, we have

$$f_{Tu}^p = 0.020 \pm 0.004, \qquad f_{Td}^p = 0.026 \pm 0.005,$$
$$f_{Ts}^p = 0.118 \pm 0.062. \tag{28}$$

The expression for f^n can be easily obtained taking into account that $f_{Tu}^n = f_{Td}^p$, $f_{Td}^n = f_{Tu}^p$ and $f_{Ts}^n = f_{Ts}^p$. We then can write the Wimp-nucleon scalar cross section that is useful for comparison with experimental results as

$$\left(\frac{d\sigma_{\text{Wimp-nucleon}}}{dE_R}\right)_{SI} = \frac{m_N \sigma_{p,n}}{2\mu_{p,n}^2 v^2} \frac{[Zf^p + (A-Z)f^n]^2}{(f^{p,n})^2} F^2(E_R), \tag{29}$$

where $F^2(E_R)$ is the nuclear form factor, E_R is the nucleus recoil energy, v is the WIMP velocity, $\mu_{p,n}$ is the WIMP-nucleon reduced mass, and $\sigma_{p,n}$ is given by

$$\sigma_{p,n} = \frac{4\mu_{p,n}^2}{\pi} (f^{p,n})^2. \tag{30}$$

For detailed steps leading to the cross section in Eq. (29) above, we indicate Refs. [7,50,60].

Once again, in order to perform the numerical computation and obtain the elastic scattering WIMP-nucleon cross section for the S331RHν model, we use the numerical package micrOMEGAS [50,51]. We present our results in Fig. 5 in the plane WIMP-nucleon cross section vs WIMP mass. In this plot, the yellow line represents the upper bound on the CDM cross section provided by LUX [6]; again, we use the complementary abundance constraints. The region in light green is overabundant, light blue is underabundant, and blue are in agreement with the cosmological CDM abundance. Here, we included the same benchmark points presented in Table I. Observe that the blue dots follow the resonance regions mentioned before. It is also important to emphasize that the direct detection puts the following lower bound on the $\tilde{\nu}_R$ mass ($m_{\tilde{\nu}_R} \geq 400$ GeV).

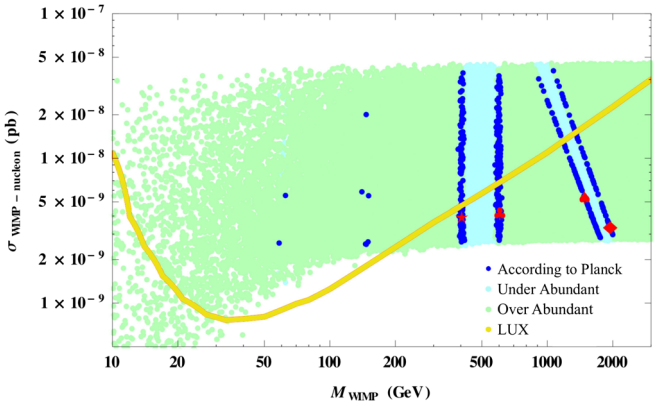

FIG. 5. WIMP-nucleon cross section vs dark matter mass. In this plot, the green points indicate overabundance, the blue points are those in agreement with the Planck bounds, and light blue points correspond to an abundance lower than needed to explain all CDM. All points above the yellow curve are excluded by direct detection from LUX [6].

As our last result, we obtain the constraint coming from CDM observables on the Z' mass. The results are presented in Fig. 6. The gray points are ruled out by LUX [6], while the green points lie in the allowed region of the parameter space. The blue points provide the observed values for the CDM relic density from Planck [2]. As we can see, the LUX constraints on the elastic WIMP-nucleon scattering cross section along with the correct relic density observed by Planck are able to establish a lower bound on the Z' mass, $m_{Z'} \gtrsim 2400$ GeV, compatible with a model-independent analysis performed in Ref. [61] as well as a particular $3-3-1$ model with left-handed neutrinos in the leptonic triplet [62]. Besides, this result is close to LHC constraints on a non-SUSY 331 model with right-handed neutrinos that impose Z' mass to lie above $M_{Z'} \gtrsim$ 2200 GeV [63], which can be further investigated in the context of the S331RHν in future work.

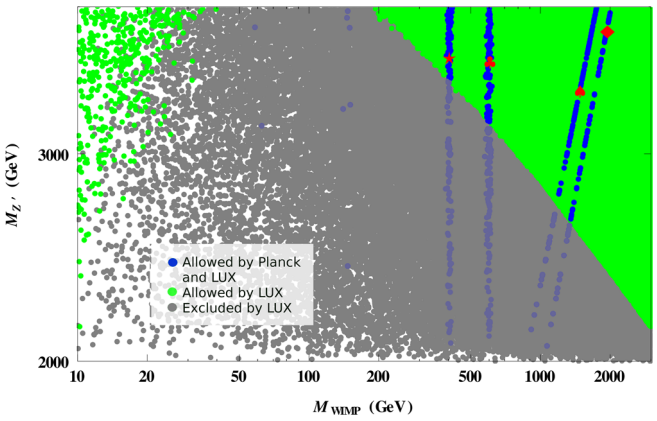

FIG. 6. Z' mass vs WIMP mass. The blue points furnish the correct abundance as indicated by Plank [2]. The green region is in agreement with recent direct-detection experiment LUX [6], and the gray region is excluded by it.

V. CONCLUSIONS

We have built a SUSY version of the gauge $SU(3)_c \otimes SU(3)_L \otimes U(1)_X$ model with right-handed neutrinos with three scalar triplets, the S331RHν model. Our first aim was to show that a Higgs boson mass of 125 GeV can be obtained without the tight bounds on stop mass and soft trilinear coupling, usually required in MSSM versions. Since our model was able to generate a tree-level Higgs mass between 80 and almost 100 GeV, the loop corrections coming from stops were alleviated, demanding a stop mass as low as 200 GeV at one-loop leading order and never much higher than 1 TeV for extremely low (close to zero) soft trilinear coupling. By itself, that is already an appealing motivation to develop this model.

We also enjoyed the opportunity to investigate the right-handed sneutrino, $\tilde{\nu}_R$, as a CDM candidate since the model has it for free in its particle multiplets. The $\tilde{\nu}_R$ in this kind of gauge model was never studied as a WIMP; only scarcely the neutralinos were considered and in a rather different version of this model as a matter of fact [57], although these are a little more intricate here as it involves a mixing of 15 neutral particles. Then, the S331RHν model offers two possibilities of WIMPs, but we concentrated on sneutrinos because they are simpler to handle than neutralinos, besides being a natural possibility in this model, not easy to attain in every SUSY model. We have computed the relic abundance of the sneutrino, contrasted with Plank observed CDM density, and direct-detection bounds from LUX experiment. We have analyzed a large portion of the parameter space, highlighting some benchmark points, and our results have shown that $\tilde{\nu}_R$ is a viable WIMP if its mass is above 400 GeV, which makes it a very interesting WIMP to be searched at the LHC.

Finally, since the right-handed sneutrino couples to a new neutral gauge bozon, Z', we pushed our CDM search to put some bounds on Z' mass. Assuming that $\tilde{\nu}_R$ is the only CDM component (or at least the one that corresponds to almost all CDM observed), the Planck results together with LUX exclusion plots allowed us to impose a bound on the plane WIMP mass against the Z' mass, implying a lower bound $M_{Z'} \gtrsim 2400$ GeV, in consonance with existing bounds on the nonsupersymmetric version of this model coming from LHC searches on Z'.

All of this constitutes interesting outcomes of this supersymmetric model that contains several theoretical features to be further explored, besides being phenomenologically testable at the LHC, as well as current experiments on CDM direct and indirect detection, which we intend to explore soon.

ACKNOWLEDGMENTS

The authors would like to thank Alexandre Alves for a careful reading of the manuscript and useful suggestions and J. G. Ferreira, Jr., and Jamerson Rodrigues for useful discussions. This work was supported by Conselho Nacional de Pesquisa e Desenvolvimento Científico–CNPq (C. A. S. P, P. S. R. S., and C. S.) and Coordenação de Aperfeiçoamento de Pessoal de Nível Superior–CAPES (A. C. O. S.).

APPENDIX: RELEVANT INTERACTIONS

The relevant interaction terms involving the R-sneutrino, Higgs, and Z' that matter for the calculation of abundance and scatter cross sections are given by

$$\mathcal{L} \supset -\frac{g\sqrt{3+t^2}}{3}\tilde{\nu}_R^\dagger(\partial^\mu\tilde{\nu}_R)Z'_\mu - \frac{1}{18}\sum_j \lambda_j \tilde{\nu}_R^\dagger S_j \tilde{\nu}_R, \quad \text{(A1)}$$

where

$$\lambda_j = g(a_{1j}(-3+2t^2)v_{\eta_1} - a_{2j}(3+2t^2)v_{\eta'_1} - a_{3j}(3+4t^2)v_\rho + a_{4j}(-3+4t^2)v_{\rho'}), \quad \text{(A2)}$$

with $j = 1, 2, 3, 4$ and $S_j = H', h', H, h$, respectively. The coefficients a_{ij} are the mixing parameters involving the Higgs. They are calculated numerically.

The other set of relevant interactions for our calculations is those involving quarks, leptons, and Z' provided by the Lagrangian

$$\mathcal{L} \supset i\sum_f \overline{f}\gamma^\mu(g_{l.h.}^{fZ'}P_L + g_{r.h.}^{fZ'}P_R)fZ'_\mu + \sum_{f,j}\lambda_f \overline{f} S_j f, \quad \text{(A3)}$$

where $j = 1, 2, 3, 4$ with $S_j = H', h', H, h$, respectively, and $P_{R,L} = \frac{1}{2}(1 \pm \gamma_5)$. The couplings $g_{l.h.}^{fZ'}$, $g_{r.h.}^{fZ'}$, and λ_f are given by Table II, and the parameters M_e and M_q are the physical masses of charged leptons and quarks, respectively.

TABLE II. Z' and scalars couplings of Eq. (A3).

Fermions (f)	$g_{l.h.}^{fZ'}$	$g_{r.h.}^{fZ'}$	λ_f
e_i	$-\frac{g(3-2t^2)}{12\sqrt{3+t^2}}$	$\frac{6gt^2}{12\sqrt{3+t^2}}$	$-\frac{2a_{4j}M_{e_i}}{v_{\rho'}}$
ν_{Ri}	$-\frac{g(3-2t^2)}{12\sqrt{3+t^2}}$	0	0
u, c	$\frac{3g}{12\sqrt{3+t^2}}$	$-\frac{4gt^2}{12\sqrt{3+t^2}}$	$-\frac{2a_{3j}M_{u,c}}{v_\rho}$
d, s	$\frac{3g}{12\sqrt{3+t^2}}$	$\frac{2gt^2}{12\sqrt{3+t^2}}$	$-\frac{2a_{1j}M_{d,s}}{v_{\eta_1}}$
b	$-\frac{g(3+2t^2)}{12\sqrt{3+t^2}}$	$\frac{2gt^2}{12\sqrt{3+t^2}}$	$-\frac{2a_{4j}M_b}{v_{\rho'}}$
t	$-\frac{g(3+2t^2)}{12\sqrt{3+t^2}}$	$-\frac{4gt^2}{12\sqrt{3+t^2}}$	$-\frac{2a_{2j}M_t}{v_{\eta'_1}}$

[1] G. Hinshaw *et al.* (WMAP Collaboration), Astrophys. J. Suppl. Ser. **208**, 19 (2013).
[2] P. A. R. Ade *et al.* (Planck Collaboration), arXiv: 1502.01589.
[3] R. Agnese *et al.* (CDMS Collaboration), Phys. Rev. Lett. **111**, 251301 (2013).
[4] E. Aprile *et al.* (XENON100 Collaboration), Phys. Rev. Lett. **109**, 181301 (2012).
[5] F. Reindl *et al.* (CRESST Collaboration), 12th Conference on the Intersections of Particle and Nuclear Physics (CIPANP 2015) Vail, Colorado, 2015 (unpublished).
[6] D. S. Akerib *et al.* (LUX Collaboration), Phys. Rev. Lett. **116**, 161301 (2016).
[7] G. Jungman, M. Kamionkowski, and K. Griest, Phys. Rep. **267**, 195 (1996).
[8] G. Bertone, D. Hooper, and J. Silk, Phys. Rep. **405**, 279 (2005).
[9] J. S. Hagelin, G. L. Kane, and S. Raby, Nucl. Phys. **B241**, 638 (1984).
[10] L. E. Ibanez, Phys. Lett. **137B**, 160 (1984).
[11] T. Falk, K. A. Olive, and M. Srednicki, Phys. Lett. B **339**, 248 (1994).
[12] T. Asaka, K. Ishiwata, and T. Moroi, Phys. Rev. D **73**, 051301 (2006).
[13] S. Gopalakrishna, A. de Gouvea, and W. Porod, J. Cosmol. Astropart. Phys. 05 (2006) 005.
[14] T. Asaka, K. Ishiwata, and T. Moroi, Phys. Rev. D **75**, 065001 (2007).
[15] H.-S. Lee, K. T. Matchev, and S. Nasri, Phys. Rev. D **76**, 041302 (2007).
[16] C. Arina and N. Fornengo, J. High Energy Phys. 11 (2007) 029.
[17] D. G. Cerdeno, C. Munoz, and O. Seto, Phys. Rev. D **79**, 023510 (2009).
[18] D. G. Cerdeno and O. Seto, J. Cosmol. Astropart. Phys. 08 (2009) 032.
[19] G. Belanger, M. Kakizaki, E. K. Park, S. Kraml, and A. Pukhov, J. Cosmol. Astropart. Phys. 11 (2010) 017.
[20] G. Belanger, J. Da Silva, and A. Pukhov, J. Cosmol. Astropart. Phys. 12 (2011) 014.
[21] B. Dumont, G. Belanger, S. Fichet, S. Kraml, and T. Schwetz, J. Cosmol. Astropart. Phys. 09 (2012) 013.
[22] V. De Romeri and M. Hirsch, J. High Energy Phys. 12 (2012) 106.
[23] Y.-L. Tang and S.-h. Zhu, Phys. Rev. D **93**, 095006 (2016).
[24] M. Singer, J. W. F. Valle, and J. Schechter, Phys. Rev. D **22**, 738 (1980).
[25] R. Foot, H. N. Long, and T. A. Tran, Phys. Rev. D **50**, R34 (1994).
[26] J. C. Montero, F. Pisano, and V. Pleitez, Phys. Rev. D **47**, 2918 (1993).
[27] F. Pisano and V. Pleitez, Phys. Rev. D **46**, 410 (1992).
[28] P. H. Frampton, Phys. Rev. Lett. **69**, 2889 (1992).
[29] C. A. de Sousa Pires and O. P. Ravinez, Phys. Rev. D **58**, 035008 (1998); **58**, 035008 (1998).
[30] P. B. Pal, Phys. Rev. D **52**, 1659 (1995).
[31] A. G. Dias and V. Pleitez, Phys. Rev. D **69**, 077702 (2004).
[32] A. G. Dias, C. A. de S. Pires, and P. S. R. da Silva, Phys. Rev. D **68**, 115009 (2003).
[33] A. Gusso, C. A. de S. Pires, and P. S. Rodrigues da Silva, Mod. Phys. Lett. A **18**, 1849 (2003).
[34] A. G. Dias, C. A. de S. Pires, and P. S. Rodrigues da Silva, Phys. Lett. B **628**, 85 (2005).
[35] D. Cogollo, H. Diniz, C. A. de S. Pires, and P. S. Rodrigues da Silva, Eur. Phys. J. C **58**, 455 (2008).
[36] F. Queiroz, C. A. de S. Pires, and P. S. R. da Silva, Phys. Rev. D **82**, 065018 (2010).
[37] C. A. d. S. Pires, arXiv:1412.1002.
[38] C. A. de S. Pires and P. S. Rodrigues da Silva, J. Cosmol. Astropart. Phys. 12 (2007) 012.
[39] J. K. Mizukoshi, C. A. de S. Pires, F. S. Queiroz, and P. S. Rodrigues da Silva, Phys. Rev. D **83**, 065024 (2011).
[40] J. D. Ruiz-Alvarez, C. A. de S. Pires, F. S. Queiroz, D. Restrepo, and P. S. Rodrigues da Silva, Phys. Rev. D **86**, 075011 (2012).
[41] P. S. Rodrigues da Silva, arXiv:1412.8633.
[42] C. Kelso, C. A. de S. Pires, S. Profumo, F. S. Queiroz, and P. S. Rodrigues da Silva, Eur. Phys. J. C **74**, 2797 (2014).
[43] F. S. Queiroz, AIP Conf. Proc. **1604**, 83 (2014).
[44] J. C. Montero, V. Pleitez, and M. C. Rodriguez, Phys. Rev. D **65**, 035006 (2002).
[45] J. C. Montero, V. Pleitez, and M. C. Rodriguez, Phys. Rev. D **70**, 075004 (2004).
[46] P. V. Dong, D. T. Huong, M. C. Rodriguez, and H. N. Long, Eur. Phys. J. C **48**, 229 (2006).
[47] P. V. Dong, D. T. Huong, M. C. Rodriguez, and H. N. Long, Nucl. Phys. **B772**, 150 (2007).
[48] H. N. Long, Phys. Rev. D **54**, 4691 (1996).
[49] W. H. Press, S. A. Teukolsky, W. T. Vetterling, and B. P. Flannery, *Numerical Recipes: The Art of Scientific Computing*, 3rd ed. (Cambridge University Press, New York, 2007).
[50] G. Belanger, F. Boudjema, A. Pukhov, and A. Semenov, Comput. Phys. Commun. **180**, 747 (2009).
[51] G. Belanger, F. Boudjema, A. Pukhov, and A. Semenov, Comput. Phys. Commun. **185**, 960 (2014).
[52] T. Hahn, S. Heinemeyer, W. Hollik, H. Rzehak, and G. Weiglein, Phys. Rev. Lett. **112**, 141801 (2014).
[53] L. J. Hall, D. Pinner, and J. T. Ruderman, J. High Energy Phys. 04 (2012) 131.
[54] P. Fileviez Prez and S. Spinner, Phys. Rev. D **87**, 031702 (2013).
[55] T. V. Duong and E. Ma, Phys. Lett. B **316**, 307 (1993).
[56] H. N. Long, Adv. Stud. Theor. Phys. **4**, 173 (2010).
[57] D. T. Huong and H. N. Long, J. High Energy Phys. 07 (2008) 049.
[58] A. Semenov, Comput. Phys. Commun. **201**, 167 (2016).
[59] A. Belyaev, N. D. Christensen, and A. Pukhov, Comput. Phys. Commun. **184**, 1729 (2013).
[60] G. Bertone, *Particle Dark Matter: Observations, Models and Searches* (Cambridge University Press, Cambridge, England, 2010).
[61] A. Alves, A. Berlin, S. Profumo, and F. S. Queiroz, Phys. Rev. D **92**, 083004 (2015).
[62] S. Profumo and F. S. Queiroz, Eur. Phys. J. C **74**, 2960 (2014).
[63] Y. A. Coutinho, V. Salustino Guimarães, and A. A. Nepomuceno, Phys. Rev. D **87**, 115014 (2013).